ACS APPLIED MATERIALS & INTERFACES

Research Article

www.acsami.org

Ruthenium Complex Containing Block Copolymer For the Enhancement of Carbon Nanotube Photoconductivity

Chi Ho Li,[†] Alan Man Ching Ng,[‡] Chris S. K. Mak,[†] Aleksandra B. Djurišić,[‡] and Wai Kin Chan*[,†]

[†]Institute of Molecular Functional Materials, Department of Chemistry, and [‡]Department of Physics, The University of Hong Kong, Pokfulam Road, Hong Kong

Supporting Information

ABSTRACT: We report the synthesis of a multifunctional block copolymer incorporated with pyrene and ruthenium terpyridyl thiocyanato complex moieties by reversible addition−fragmentation chain transfer polymerization. The pyrene block in the copolymer facilitates the dispersion of multiwalled carbon nanotubes in DMF solution because of the strong $\pi-\pi$ interaction between the pyrene moieties and nanotube surface. On the other hand, the ruthenium complexes greatly enhance the photosensitivity of the functionalized nanotubes in the visible region. The photocurrent responses of the nanotubes at different wavelength measured by conductive AFM spectrum strongly agree with the absorption spectrum of the ruthenium complex. The results demonstrate a new and versatile approach in enhancing and fine-tuning the photosensitivity or other opto-electronic properties of carbon nanotubes by multifunctional block copolymers.

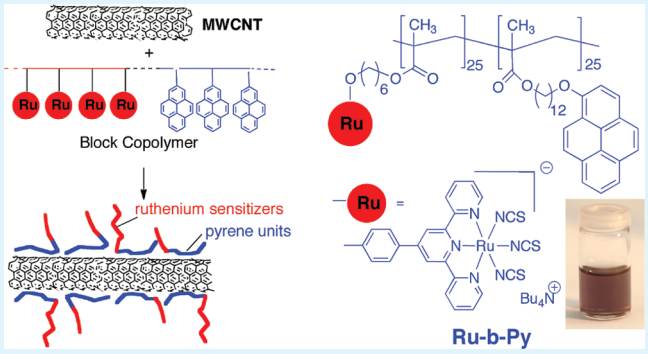

KEYWORDS: *block copolymers, controlled radical polymerization, carbon nanotubes, organic electronics, photoconductivity*

INTRODUCTION

The application of carbon nanotubes (CNTs) in electronic and optoelectronic devices has drawn tremendous attention in recent years.[1] CNTs may function as conductors with very high conductivity, but their electronic properties are strongly affected by the introduction of different functional groups/molecules on the surface. The type of charge carriers can be easily modified by the surface functionalization, which is equivalent to n-doping and p-doping in semiconductors.[2] Composites based on CNTs have been applied in electronic and optoelectronic devices[3] such as field effect transistors (FET),[4,5] photoswitching,[6] light sensing,[7] chemical sensing,[8] and light emitters.[9] Organic chromophores[7] or conjugated polymers[10,11] have been used to modify the optical properties of CNT. Photovoltaic devices based on CNT modified with conjugated P3HT were also reported.[12] In these applications, chemical modification and functionalization are essential, as the responses of CNTs to different stimuli are dependent on the molecules/groups attached.[13,14] In most of the devices fabricated from CNTs, the sensitizing molecules were introduced to the "as grown" nanotube surface by dropping a solution of the sensitizers on the substrate on which CNT was formed. The nanotube surface may not be fully covered, and small molecules usually have weak interactions with CNT surface. This may result in detachment of molecules upon subsequent washing/cleaning processes. Another approach to functionalize CNT surface is by the formation covalent linkage after modifying CNT surface by chemical methods. For example, carboxylic acid groups can be introduced to CNT surface by treating with oxidizing agents.[15] However, the continuous π-system of CNTs will effectively be destroyed.[16] Different approaches in noncovalent functionalization of carbon nanotubes have been proposed.[17] The noncovalent interaction between the anchoring group and CNT was mainly based on $\pi-\pi$ interaction. Anthracene, pyrene, porphyrin, and phthalocyanine derivatives have been used as the anchoring groups.

We previously demonstrated that metal containing block copolymers and conjugated polymers could function as photosensitizers in photovoltaic devices.[18,19] In these applications, the metal complex sensitizers played critical role in the generation of photocurrent by broadening the absorption spectra in the visible to near IR region.[20,21] CNTs modified with a variety of block copolymers have been reported.[22,23] In this paper, we report a new approach in modifying the surface of CNT with a photosensitizing metal containing block copolymer that contains pyrene moieties in one block and ruthenium terpyridyl thiocyanato complexes in another block. The ruthenium complex is commonly known as the black dye, and it has been widely used as photosensitizers in dye-sensitized solar cells.[24] In our copolymer, the two different blocks serve distinct functions: the pyrene block facilitates the

Received: May 12, 2011
Accepted: November 25, 2011
Published: December 9, 2011

   dx.doi.org/10.1021/am201561g | ACS Appl. Mater. Interfaces 2012, 4, 74−80

Scheme 1. Synthesis of Ru-b-Py

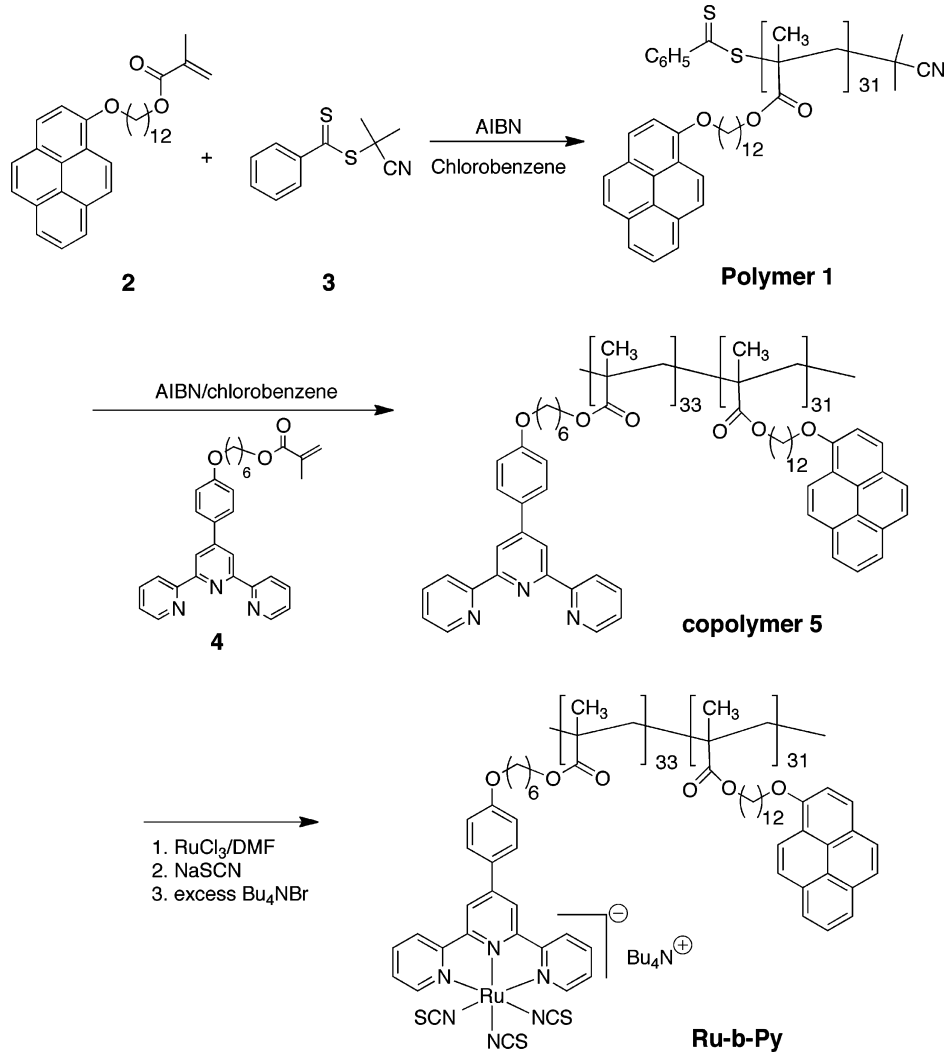

anchorage of the copolymer on CNT surface by noncovalent $\pi-\pi$ interactions, so that the modified CNT can be dispersed easily in common organic solvents. The ruthenium complex block absorbs strongly in the visible region and functions as photosensitizer. After modification, the CNT will be wrapped with pyrene containing block in the inner layer, whereas the ruthenium complexes constitute the outer layer of the modified CNT. By this approach, the noncovalent attachment of molecules on CNT surface does not result in perturbation of CNT electronic states.[16] In addition, compared to small molecules, the block copolymer can anchor on CNT surface much more strongly, and it may serve as a dispersing agent for CNT. Because of the presence of photosensitizing block, the photoconductivity of CNT was enhanced after functionalization. The resulting CNT−polymer composite have potential applications in organic photovoltaic devices.[25] Here, we present a simple and convenient technique by which the photoconductivity of an individual functionalized carbon nanotube can be directly measured by conductive AFM (CAFM) under illumination of light.

RESULTS AND DISCUSSION

Synthesis of Copolymer and Dispersion of CNT. The synthesis of the target block copolymer **Ru-b-Py** is shown in Scheme 1. It was synthesized by the reversible addition−fragmentation chain transfer polymerization (RAFT). Similar procedure has been adopted in the synthesis of photosensitizing block copolymers.[18] The pyrene containing block was synthesized by heating monomer **2** in the presence of AIBN as the initiator and cyanoisopropyldithiobenzoate **3** as the chain transfer agent. The product obtained (polymer **1**) was used as the macroinitiator for the synthesis of the second block. The GPC chromatograms of different homopolymer and copolymers are shown in Figure 1 and the calculated and measured molecular weights are summarized in Table 1. The number average molecular weight and polydispersity measured for polymer **1** were 14570 and 1.08, respectively (by GPC using NMP-4% KPF_6 as the eluent). This corresponds to a number average degree of polymerzation of 31. The measured molecular weight agrees very well with that of theoretical value (11750, assuming that [monomer]/[chain transfer reagent] = 25). In the second step, metal free block copolymer **5** was synthesized by the reaction between monomer **4** and macroinitiator **1**. The GPC trace of copolymer **5** shows no residual polymer **1** in the mixture., and the number avarage molecular weight measured was 30800 (degee of polymerization = 33), which also agrees quite well with the theoretical value (29850). It can be seen that both polymers **1** and **5**

dx.doi.org/10.1021/am201561g | ACS Appl. Mater. Interfaces 2012, 4, 74−80

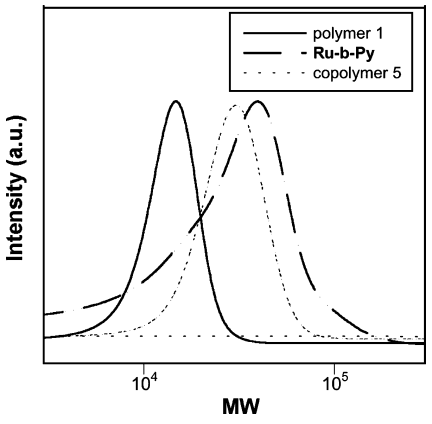

Figure 1. GPC chromatograms of polymers **1**, **5**, and **Ru-b-Py** on refractive index detector. The eluent was NMP with 4% KPF_6.

Table 1. Characterizations of Polymers

sample	M_n (calcd)[a]	M_n (expt)[b]	polydispersity[b]
polymer **1**	11750	14570	1.08
copolymer **5**	29850	30800	1.14
Ru-b-Py	45750	33170	1.30

[a]The theoretical molecular weight was estimated from the molar ratio between the chain transfer reagent to the monomer. For **Ru-b-Py**, the value was calculated by assuming that all the terpyridine ligands formed coordinated ruthenium complexes. [b]Measured by GPC.

exhibit low polydispersity, indicating the "living" nature of the polymerizations. For the metalation reaction, copolymer **5** was first heated with ruthenium trichloride in DMF. In this reaction, the intermediate obtained was not soluble in DMF, and it limited the percentage of trichloro ruthenium moieties incorporated in the polymer. The chloride ligands on the ruthenium center were then replaced by thiocyanate by heating the intermediate polymer with sodium thiocyanate in DMF. Subsequently, the sodium ion was replaced by tetrabutylammonium cation to yield the target polymer **Ru-b-Py**, which is highly soluble in DMF. The GPC chromatogram of **Ru-b-Py** shows a significant peak broadening compared with the metal free copolymer **5**, and the measured molecular weight is lower than that of the theoretical value, which assumes a 100% metalation. It should be noted that **Ru-b-Py** consists of ionic ruthenium complex pendant chain, and this type of polymer may bahave differently compared to neutral polymers. The formation of aggregates, strong polymer-column interactions,[26] and incomplete metalation may contribute to the broadening of the GPC peak. The ^{1}H NMR spectra of polymers **1**, **5** are shown in Figure S1 (see the Supporting Information) and the spectra of the monomers are also shown for comparison purpose. By comparing the spectra of monomer **2** and polymer **1**, the peak at ca. 8.3 ppm is assigned to the protons on the pyrene moiety. For copolymer **5**, the peaks at ca. 8.5−8.7 and 6.8−6.9 ppm are assigned to the protons of the terpyridine unit. By comparing the integrals of the peaks from the pyrene and terpyridine moieties, the block size ratio in copolymer **5** can be calcuated, and the result (1.2) is very close to that obtained from GPC. After introducing ruthenium thiocyanate complex to the terpyridine block, **Ru-b-Py** shows additional broad peaks at ca. 0.9−1.8 ppm due to the tetrabutylammonium cation, while other specteal features are similar to the metal free copolymer **5**. From the elemental analysis results, it was estimated that 75% of the terpyridine units were functionalized with ruthenium complexes. EDX results confirmed the Ru to S ratio to be 1:3, showing complete substitution of the chloride by thiocyanate ligands.

The UV−vis absorption spectra of polymer **1**, **Ru-b-Py**, and multiwalled CNT modified with **Ru-b-Py** are shown in Figure

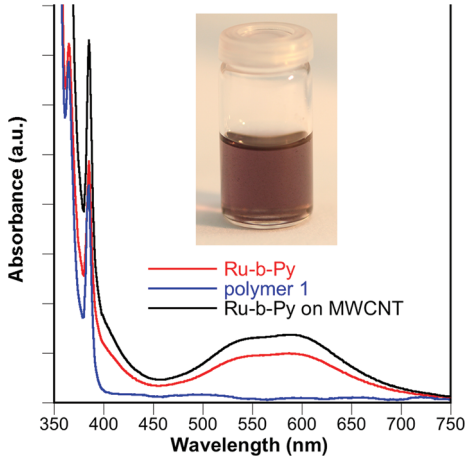

Figure 2. UV−vis absorption spectra of polymer **1**, **Ru-b-Py**, and carbon nanotube functionalized with **Ru-b-Py** measured in DMF solution. The inset figure shows a solution of CNT modified with **Ru-b-Py** in DMF solution two days after dispersion.

2. All the polymers show two sharp and intense absorption peaks at 364 and 385 nm, which are assigned to the $\pi-\pi^*$ absorption of the pyrene moieties. After metal complexation, **Ru-b-Py** shows a very broad absorption band in the range between 450 and 700 nm, which is assigned to the absorption by the ruthenium complex moieties. Compared to ruthenium bisterpyridyl complexes, the red shift in this metal-to-ligand charge transfer transition is due to the electron donation from the thiocyanate ligand to ruthenium center, resulting in stabilization of the excited states. This is consistent to the electronic transitions observed in other ruthenium thiocyanate complexes.[24] The modification of CNT surface was carried out by ultrasonicating a DMF solution of **Ru-b-Py** in the presence of multiwalled CNTs. After removing excess polymer by filtration with a membrane filter (0.2 μm) and washing with solvent, the CNT sample was redispersed in DMF solution again. No sedimentation of solid was observed within 5 days, indicating the formation of a homogeneous and stable suspension of nanotubes (Figure 2, inset). A schematic diagram showing the functionalization of CNT surface is shown in Figure 3. Pyrene is known to have strong noncovalent interaction with CNT surface. After functionalization, the CNT-polymer composite can be dispersed in DMF easily, which strongly suggests that the surface of the CNT has been modifed by polar/ionic functional groups. Therefore, it is reasonable to conclude that the CNT surface was covered by the pyrene block, whereas the "outer" part of the tube is mainly composed of the ruthenium complex. It can be seen that the absorption spectrum of the resulting **CNT-Ru-b-Py** suspension is almost identical to the original block copolymer **5** (Figure 2), indicating that CNTs have little contribution to the optical absorption.

Figure 4a shows the TEM micrograph of a MWCNT functionalized with **Ru-b-Py**. The sample was not stained, and the contrast observed on the nanotube surface is mainly due to the presence of ruthenium in the copolymer. It can clearly be

dx.doi.org/10.1021/am201561g | ACS Appl. Mater. Interfaces 2012, 4, 74−80

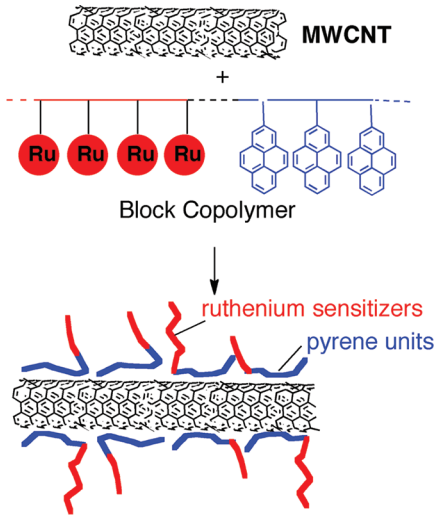

Figure 3. Schematic diagram showing the functionalization of CNT surface with **Ru-b-Py**.

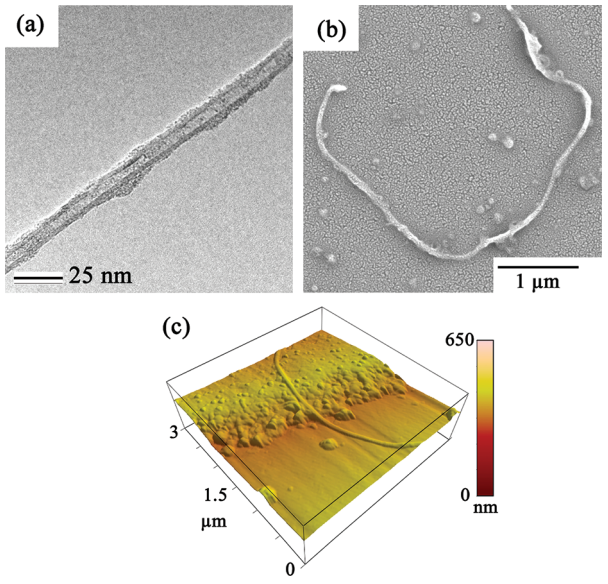

Figure 4. (a) TEM micrograph CNT functionalized with **Ru-b-Py**. (b) SEM micrograph of CNT functionalized with **Ru-b-Py** deposited on a silicon wafer substrate. (c) AFM topographical image of the functionalized CNT position at the edge of an ITO electrode.

seen that the a layer of amorphous material is coated on the surface of the nanotube, and the thickness of is approximately 3−5 nm. EDX experiment confirmed the presence of ruthenium in the material, and the ruthenium to sulfur ratio on CNT surface was consistent to the ruthenium thiocyanate complex in the block copolymer. This strongly suggests that the ruthenium complex block constitutes the outer surface of the functionalized CNT, whereas the pyrene blocks are in contact with the CNT surface. Figure 4b shows the SEM micrograph of an individual functionalized CNT. Most of the functionalized CNTs exist as individual tubes, and no significant aggregation was observed. This demonstrates the effective dispersion of CNTs by the block copolymer. Figure 4c shows the AFM micrograph of a functionalized CNT positioned right at the edge of an ITO electrode. The diameters of modified CNTs measured by both TEM and AFM are consistent with each other.

Photocurrent Measurements. In the literature, the photosensitizing properties of CNTs were studied by measuring the drain current of an FET in which the nanotube was placed across the source and drain electrodes.[27] Although the current measured can be greatly enhanced by the increase in gate voltage, the device fabrication requires tedious procedure and equipment such as e-beam lithography and metal deposition. In this work, we used a CAFM equipped with a second microprobe, which was made contact with the patterned ITO electrodes. One of the challenges in measuring the electrical properties of CNT with CAFM is that the position of nanotube may shift when the cantilever was moved across the nanotube. Before dispersing the nanotube samples, the substrate surface was modified with a layer of 3-aminopropyltrimethoxysilane. It was found that the mobility of functionalized CNT on the modified substrate surface was reduced after the surface treatment, and the position of nanotube did not change when the AFM probe was moved across the sample. This may be due to the stronger interaction between the anionic ruthenium trithiocyanate complex and the amino groups introduced to the substrate surface. Although this surface treatment may only be specific to CNT functionalized with ionic functionalities, we observed that the mobility of CNT functioalized with polymer **1** also decreased when dispersed on the pretreated ITO. Therefore, other factors may also contribute to the reduction in mobility. After surface treatment, diluted nanotube dispersion was introduced on the ITO substrate by drop casting. The sample was studied with AFM to identify the position of a CNT that was located at the edge of an ITO electrode. Once such nanotube was identified, a microprobe was placed on the ITO electrode. The schematic diagram of the experimental setup is shown in Figure 5. A

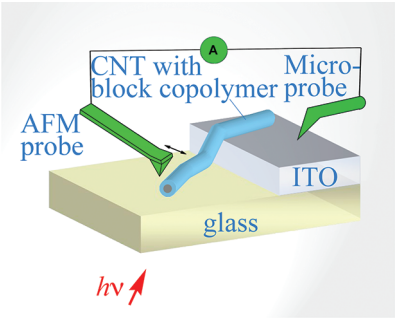

Figure 5. Schematic diagram showing the measurement of photocurrent response of the functionalized CNT by conductive AFM.

conductive AFM probe was positioned at the other end of the tube at which no ITO was present underneath. The distance between the CAFM probe and the ITO electrode was kept at 1 μm for all measurement in order to eliminate the effect due to the tube length. A bias was applied across the microprobe and the CAFM probe, and the current passing through the nanotube was measured when the CAFM probe moved across the nanotube. In essence, an electric field was applied parallel to the orientation of the nanotube. Current measurement was performed both under dark and illumination with light from the bottom of the substrate with different wavelengths.

Figure 6 shows the current voltage response of the nanotube coated with **Ru-b-Py** under dark and illumination with light (λ = 532 nm). Both *IV* curves show symmetric and nonlinear current response under forward and reverse bias. Strong

dx.doi.org/10.1021/am201561g | *ACS Appl. Mater. Interfaces* 2012, 4, 74−80

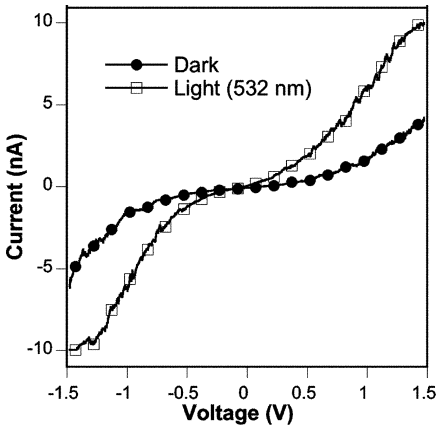

Figure 6. Current−voltage characteristics of CNT functionalized with **Ru-b-Py** under dark and illumination with light (wavelength = 532 nm, intensity = 1.3 μW/cm^2).

enhancement in current was observed when the sample was illuminated. In order to investigate the origin of photosensitization, the sample was illuminated by different wavelength of light. The photocurrent responses (bias = 1.0 V) of CNT modified with polymer **1** and **Ru-b-Py** as the function of incident light wavelength are shown in Figure 7. The

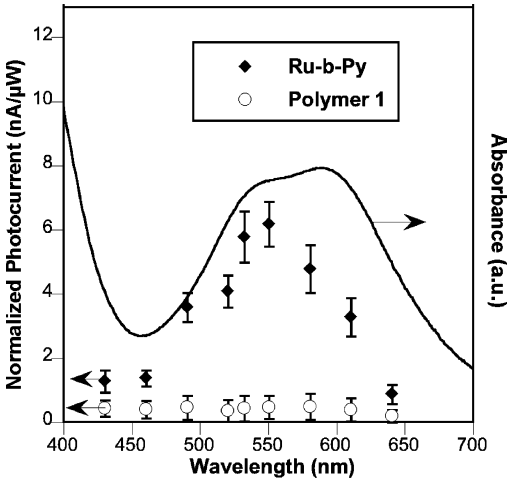

Figure 7. Photocurrent response (after normalized by incident light intensity) of CNTs functionalized with polymer **1** and **Ru-b-Py** at different wavelength. The error bars show the standard derivations of results from three measurements.

absorption spectrum of CNT coated with **Ru-b-Py** is also shown for comparison. The photocurrents were calculated by subtracting the current measured by the dark current measured under the same condition, and were normalized by correcting the difference in light intensity at different wavelengths. It was reported that the photocurrent spectra of CNT showed a maximum in the near-infrared region.[28] For CNT functionalized with polymer **1**, the photcurrent measured was quite small and the magnitude is similar in the entire visible region. This is mainly attributed to the absorption by the CNT. For CNT functionalized with **Ru-b-Py**, it can be seen that the photocurrent responses agree quite well with the absorption spectrum of the ruthenium complex. Therefore, the photocurrent maximum of our copolymer modified CNT observed at ca. 550 nm is mainly due to the sensitization by the ruthenium complexes, which play critical role in the generation of photo charge carriers.

The cyclic voltammograms of polymer **1** and **Ru-b-Py** are shown in Figure 8. In polymer **1**, a quasi-reversible oxidative

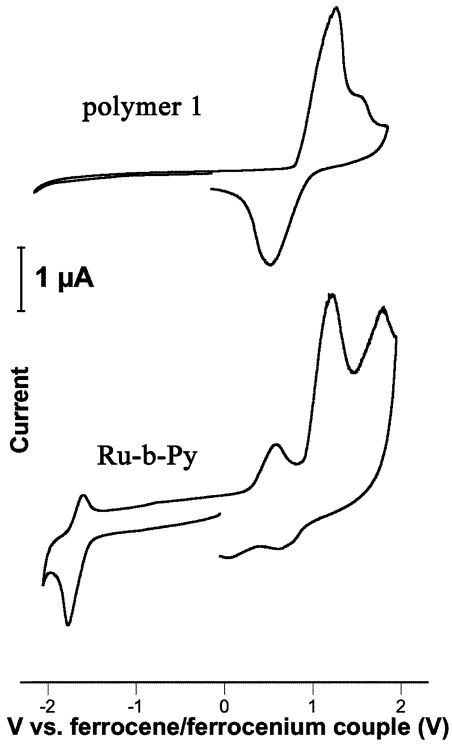

Figure 8. Cyclic voltammogram of **Ru-b-Py** measured in DMF solution. The applied bias was corrected by ferrocene internal standard. Scan rate = 50 mV/s.

wave at 1.1 V is observed, which is assigned to the oxidation of the pyrene moieties. In **Ru-b-Py**, in addition to the redox process due to pyrene, an oxidative and a reductive waves are observed at 0.6 and −1.6 V, respectively. These are assigned to the $Ru^{II/III}$ couple and ligand reduction of the ruthenium complex moieties.[24] There is another oxidative wave observed at 1.8 V. However, the origin of such oxidation is not clear. It may be due to further oxidation of the pyrene. After correction with ferrocene internal standard, the HOMO−LUMO levels were calculated to be −5.4 and −3.2 eV, respectively. It was reported that workfunction of multiwalled CNT was −4.3 eV[29,30] and the bandgap was on the order of 1 eV.[31] Therefore, after photoexcitation of the ruthenium complexes, electron transfer from the sensitizer (LUMO level = −3.2 eV) to nanotubes may occur. Subsequently, electrons generated will be transported by the highly conducting nanotube to the respective electrode. This photosensitizer-electron transport system may be a potential candidate for organic photovoltaic cells.

CONCLUSIONS

In summary, we have demonstrated the modification of carbon nanotube surface by a block copolymer functionalized with pyrene anchoring groups and ruthenium complex photosensitizers. The block copolymer could facilitate the dispersion of carbon nanotubes in organic solvents. In addition, compared to pure carbon nanotubes, the photosensitivity of the copolymer modified nanotubes can be greatly enhanced and

broadened in the visible region. The photocurrent response of individual functionalized carbon nanotube could be measured by CAFM directly. This approach allows us to design new polymer−carbon nanotube composites and to fine-tune their photosensitivity in different wavelength. The resulting copolymer−CNT composite has promising potentials to be the active materials in organic photovoltaic devices.

EXPERIMENTAL SECTION

Reagents and Materials. Pyrene, methylacryloyl chloride and borane-dimethylsulfide complex solution, were purchased from Aldrich Chemicals Co. Ruthenium trichloride hydrate was purchased from Precious Metal Online. Cyanoisopropyldithiobenzoate[33] and 4′-[4-(6-Methacryloylhexyloxy)phenyl]-2,2′:6′2″-terpyridine[18] were synthesized by previously reported procedures. Multiwalled Carbon nanotubes were purchased from NanoLab Inc. AIBN was recrystallized with ethanol before used. DMF were distilled over calcium hydride under nitrogen atmosphere before used. All the other materials were used as received. The syntheses of macroinitiator (polymer **1**) and block copolymer **Ru-b-Py** are shown in Scheme 1.

*12-(Pyren-1-yloxy)dodecyl methacrylate (**2**).* In a dried, nitrogen purged flask, 12-(pyren-1-yloxy)dodecan-1-ol (2.5 g, 6.2 mmol),[34,35] triethylamine (8.6 mL, 62 mmol) and THF (40 mL) were added. The solution was stirred under ice bath until the solid was dissolved. Methylacryloyl chloride (1.8 mL, 18.6 mmol) was added dropwise to the flask. The mixture was stirred in room temperature for 16 h. The excess solvent was removed by a rotary evaporator. The solid collected was dissolved in dichloromethane and the organic layer was washed with water twice. The organic extract was dried over magnesium sulfate. After removal of solvent, the yellow solid was washed with minimum amount of cold methanol and then further purified by silica gel column chromatography using 95:5 hexane/ethyl acetate mixtures as the eluent (Yield =47%). ^{1}H NMR (400 MHz, $CDCl_3$) δ = 8.47 (d, J = 5.2 Hz, 2H), 8.08 (s, 3H), 8.01 (d, J = 4.7 Hz, 1H), 7.95 (d, J = 4.2 Hz, 2H), 7.87 (d, J = 6.1 Hz, 1H), 7.52 (d, J = 6.4 Hz, 1H), 6.08 (s, 1H), 5.53 (s, 1H), 4.32 (t, J = 6.3 Hz, 2H), 4.11 (t, J = 6.1 Hz, 2H), 1.93 (s, 3H), 1.65 −1.60 (m, 4H), 1.54−1.25 (m, 16H). ^{13}C NMR (100 MHz, $CDCl_3$) δ = 153.4, 136.7, 131.9, 127.4, 126.4, 126.2 125.6, 125.3, 125.0, 124.3, 124.2, 121.5, 109.3, 69.1, 65.0, 29.8, 29.7, 29.6,29.5, 29.4, 28.8, 26.4, 26.1,18.5.

*Polymer **1**.* Monomer **2** (200 mg, 4.3 mmol), cyanoisopropyldithiobenzoate (4 mg, 0.17 mmol), AIBN (2 mg, 0.08 mmol) and freshly distilled chlorobenzene were added to a 10 mL ampule under nitrogen atmosphere. The resulting solution was degassed by three freeze−pump−thaw cycles and sealed under vacuum. The reaction mixture was stirred at 60 °C for 18 h. The reaction mixture was precipitated in methanol (250 mL) and the solid was collected. Purification of the product was done by repeating the precipitation procedure twice (Yield = 77%). The polymer obtained was used as the macroinitiator for subsequent polymerization reaction.

*Copolymer **5**.* Polymer **1** (200 mg), monomer 4 (64 mg, 0.13 mmol), AIBN (2.1 mg, 0.01 mmol) and freshly distilled chlorobenzene (2 mL) were added to a 10 mL ampule under a nitrogen atmosphere. The resulting solution was degassed by three freeze−pump−thaw cycles and sealed under vacuum. The reaction mixture was stirred at 60 °C for 24 h. The reaction mixture was precipitated in methanol (250 mL) and the solid was collected. Purification of the polymer was done by dissolving the polymer in chlorobenzene and reprecipitation in methanol (yield = 77%).

***Ru-b-Py*.** In a nitrogen purged, reflux condenser equipped flask, polymer 5 (200 mg), ruthenium trichloride hydrate (120 mg, 0.6 mmol) and DMF (5 mL) were added. The mixture was heated to 100 °C for 16 h and the dark solid was collected by filtration. The polymer was purified by washing with methanol in a Soxhlet extractors for 2 days. After drying in a vacuum oven, the polymer obtained (200 mg, 0.8 mmol) was introduced into a nitrogen purged, two-neck round-bottom flask. Sodium thiocyanate (0.7 g, 8 mmol) and DMF (4 mL) were added. The mixture was heated to 130 °C for 24 h under dark. After filtration, the filtrate was poured into methanol (200 mL). Tetra-*n*-butylammonium bromide was added to the solution and the precipitate formed was collected by filtration. The polymer was purified by washing with methanol in a Soxhlet extractor for 2 days. The polymer (180 mg) was collected as dark green solid, and the percentage of metal functionalization was calculated to be 75% from elemental analysis results.

Materials Characterizations. ^{1}H and ^{13}C NMR spectra were recorded on Bruker Avance-400 NMR (400 and 100 MHz respectively) and Bruker DPX-300 (300 and 75 MHz respectively) NMR spectrometers. UV−visible absorption spectra were recorded on a Varian Cary 50 UV−vis spectrometer. Mass spectra were collected on Finnigan MAT-95 mass spectrometers. Topographical Images and phase images of atomic force micrographs (AFM) were collected on an Asylum MFP3D atomic force microscope with ARC2 SPM Controller under constant temperature atmosphere. Molecular weights were determined against polystyrene standards using a Waters GPC system equipped with two Styragel HR3 and HR4 columns at 60 °C, a Waters 996 photodiode array and a Waters 2410 refractive index detectors. N-methylpyrrolidinone (NMP) with 4% potassium hexafluorophosphate was used as the eluent with a flow rate of 0.8 mL/min. Transmission Electron Microscopy (TEM) images and Energy-dispersive X-ray spectroscopy (EDX) results were collected using a Philips Tecnai G2 20 S-TWIN transmission electron microscope equipped with a INCAx-sight EDS Detectors operating at 200 kV. The samples for TEM were prepared by dispersing the sample solution (in ethanol) onto a carbon coated 400-mesh hexagonal copper grid at room temperature. Cyclic votammetry was carried out using an eDAQ EA161 potentiostat. Three mm glassy carbon electrode was used as the working electrode, silver/silver chloride electrode was used as reference electrode and Platinum wire was used as auxiliary electrode. The reference potential was calibrated with ferrocene/ferrocenium couple as an internal electrode. 0.1 M tertrabutylammonium tetrafluorobrate, in deoxygenated HPLC grade acetonitrile, was used as the supporting electrolyte.

Functionalization of Carbon Nanotubes. The dispersion of MWCNT in the presence of **Ru-b-Py** was carried out by ultrasonicating a multiwalled carbon nanotube (10 mg, Nano-Lab; OD = 15 nm, length = 5−20 μm) suspension with **Ru-b-Py** (20 mg) in DMF (20 mL) at room temperature. After filtration with a cotton filter, the solution was filtered with a PTFE membrane filter (pore size = 0.2 μm). Because of the size of the nanotubes, the nanotubes could not pass through the filter membrane. The membrane was then rinsed with DMF in order to remove the excess copolymer in the solution or on the nanotube surface. The functionalized nanotubes on the membrane surface were redispersed in solution phase again by agitating the membrane in DMF (20 mL). No sedimentation was observed in 5 days.

Photocurrent Measurements. For the photocurrent measurement, an ITO coated glass with arrays of patterned electrodes (radius = 0.5 mm) was used as the substrate. Before dispersing nanotube samples, the substrate surface was immersed in a solution of 3-aminopropyltrimethoxysilane in toluene (1%). The CNT suspension in DMF obtained as described above was diluted by 100 times with DMF. The solution was then drop cast on the patterned ITO electrode. After drying in a vacuum oven, the sample was studied with an Asylum Research ORCA conductive AFM (Ir coated ASYELEC-01 cantilever, Asylum Research). The illumination wavelength was varied by using a series of band-pass filters in the range between 400 and 700 nm, and their intensities were measured with a calibrated photodetector (Newport 818 silicon photodetector). In order to eliminate the effect of the length of nanotube, in each measurement, the distance between the conductive AFM tip and the edge of the ITO electrode was kept at 1 μm.

ASSOCIATED CONTENT

Supporting Information

^{1}H NMR spectra of different monmers and polymers. This material is available free of charge via the Internet at http://pubs.acs.org.

dx.doi.org/10.1021/am201561g | ACS Appl. Mater. Interfaces 2012, 4, 74−80

AUTHOR INFORMATION

Corresponding Author

*E-mail: waichan@hku.hk.

ACKNOWLEDGMENTS

The work described in this paper was substantially supported by a grant from the University Grants Committee of the Hong Kong Special Administrative Region, China (Project [AoE/P-03/08, HKU7005/08P]). Partial financial support from the Strategic Research Theme and University Development Fund (University of Hong Kong) is also acknowledged.

REFERENCES

(1) Léonard, F. *The Physics of Carbon Nanotube Devices*; William Andrew: Norwich, NY, 2009.
(2) Javey, A.; Kong, J., *Carbon Nanotube Electronics*; Springer: New York, 2009.
(3) Avouris, P.; Freitag, M.; Perebeinos, V. *Nat. Photon.* **2008**, *2* (6), 341−350.
(4) Hong, K.; Yang, C.; Kim, S. H.; Jang, J.; Nam, S.; Park, C. E. *ACS Appl. Mater. Inter.* **2009**, *1* (10), 2332−2337.
(5) Yun, D. J.; Hong, K.; Kim, S. H.; Yun, W. M.; Jang, J. Y.; Kwon, W. S.; Park, C. E.; Rhee, S. W. *ACS Appl. Mater. Interfaces* **2011**, *3* (1), 43−49.
(6) Guo, X. F.; Huang, L. M.; O'Brien, S.; Kim, P.; Nuckolls, C. *J. Am. Chem. Soc.* **2005**, *127* (43), 15045−15047.
(7) Hecht, D. S.; Ramirez, R. J. A.; Briman, M.; Artukovic, E.; Chichak, K. S.; Stoddart, J. F.; Gruner, G. *Nano Lett.* **2006**, *6* (9), 2031−2036.
(8) Kong, J.; Franklin, N. R.; Zhou, C. W.; Chapline, M. G.; Peng, S.; Cho, K. J.; Dai, H. J. *Science* **2000**, *287* (5453), 622−625.
(9) Misewich, J. A.; Martel, R.; Avouris, P.; Tsang, J. C.; Heinze, S.; Tersoff, J. *Science* **2003**, *300* (5620), 783−786.
(10) Shi, Y. M.; Dong, X. C.; Tantang, H.; Weng, C. H.; Chen, F. M.; Lee, C. W.; Zhang, K. K.; Chen, Y.; Wang, J. L.; Li, L. J. *J. Phys. Chem. C* **2008**, *112* (46), 18201−18206.
(11) Geng, J. X.; Kong, B. S.; Yang, S. B.; Youn, S. C.; Park, S.; Joo, T.; Jung, H. T. *Adv. Funct. Mater.* **2008**, *18* (18), 2659−2665.
(12) Berson, S.; de Bettignies, R.; Bailly, S.; Guillerez, S.; Jousselme, B. *Adv. Funct. Mater.* **2007**, *17* (16), 3363−3370.
(13) Byrne, M. T.; Gun'ko, Y. K. *Adv. Mater.* **2010**, *22* (15), 1672−1688.
(14) Peng, X. H.; Wong, S. S. *Adv. Mater.* **2009**, *21* (6), 625−642.
(15) Liu, J.; Rinzler, A. G.; Dai, H. J.; Hafner, J. H.; Bradley, R. K.; Boul, P. J.; Lu, A.; Iverson, T.; Shelimov, K.; Huffman, C. B.; Rodriguez-Macias, F.; Shon, Y. S.; Lee, T. R.; Colbert, D. T.; Smalley, R. E. *Science* **1998**, *280* (5367), 1253−1256.
(16) Satake, A.; Miyajima, Y.; Kobuke, Y. *Chem. Mater.* **2005**, *17* (4), 716−724.
(17) Herranz, M. A.; Martin, N. Noncovalent Functionalization of Carbon Nanotubes. In *Carbon Nanotubes and Related Structures*; Guldi, D. M., Martin, N., Eds.; Wiley-VCH Verlag GmbH: Weinheim, Germany, 2010; pp 103−134.
(18) Tam, W. Y.; Mak, C. S. K.; Ng, A. M. C.; Djurisic, A. B.; Chan, W. K. *Macromol. Rapid Commun.* **2009**, *30* (8), 622−626.
(19) Cheng, K. W.; Mak, C. S. K.; Chan, W. K.; Ng, A. M. C.; Djurisic, A. B. *J. Polym. Sci., Part A: Polym. Chem.* **2008**, *46*, 1305−1317.
(20) Mak, C. S. K.; Leung, Q. Y.; Li, C. H.; Chan, W. K. *J. Polym. Sci., Part A: Polym. Chem.* **2010**, *48*, 2311−2319.
(21) Mak, C. S. K.; Cheung, W. K.; Leung, Q. Y.; Chan, W. K. *Macromol. Rapid Commun.* **2010**, *31* (9−10), 875−882.
(22) Antaris, A. L.; Seo, J. W. T.; Green, A. A.; Hersam, M. C. *ACS Nano* **2010**, *4* (8), 4725−4732.
(23) Zou, J. H.; Chen, H.; Chunder, A.; Yu, Y. X.; Huo, Q.; Zhai, L. *Adv. Mater.* **2008**, *20* (17), 3337−3341.
(24) Nazeeruddin, M. K.; Péchy, P.; Grätzel, M. *Chem. Commun.* **1997**, 1705−1706.
(25) Han, J.; Kim, H.; Kim, D. Y.; Jo, S. M.; Jang, S. Y. *ACS Nano* **2010**, *4* (6), 3503−3509.
(26) Meier, M. A. R.; Lohmeijer, B. G. G.; Schubert, U. S. *Macromol. Rapid Commun.* **2003**, *24* (14), 852−857.
(27) Lee, E. J. H.; Zhi, L. J. E.; Burghard, M.; Mullen, K.; Kern, K. *Adv. Mater.* **2010**, *22* (16), 1854−1857.
(28) Freitag, M.; Martin, Y.; Misewich, J. A.; Martel, R.; Avouris, P. H. *Nano Lett.* **2003**, *3* (8), 1067−1071.
(29) Ago, H.; Kugler, T.; Cacialli, F.; Petritsch, K.; Friend, R. H.; Salaneck, W. R.; Ono, Y.; Yamabe, T.; Tanaka, K. *Synth. Met.* **1999**, *103* (1−3), 2494−2495.
(30) Ago, H.; Kugler, T.; Cacialli, F.; Salaneck, W. R.; Shaffer, M. S. P.; Windle, A. H.; Friend, R. H. *J. Phy. Chem. B* **1999**, *103* (38), 8116−8121.
(31) Blase, X.; Benedict, L. X.; Shirley, E. L.; Louie, S. G. *Phys. Rev. Lett.* **1994**, *72* (12), 1878−1881.
(32) McDonald, T. J.; Svedruzic, D.; Kim, Y. H.; Blackburn, J. L.; Zhang, S. B.; King, P. W.; Heben, M. J. *Nano Lett.* **2007**, *7* (11), 3528−3534.
(33) Thang, S. H.; Chong, Y. K.; Mayadunne, R. T. A.; Moad, G.; Rizzardo, E. *Tert. Lett.* **1999**, *40* (12), 2435−2438.
(34) Babu, P.; Sangeetha, N. M.; Vijaykumar, P.; Maitra, U.; Rissanen, K.; Raju, A. R. *Chem.—Eur. J.* **2003**, *9* (9), 1922−1932.
(35) Vyas, P. V.; Bhatt, A. K.; Ramachandraiah, G.; Bedekar, A. V. *Tert. Lett* **2003**, *44* (21), 4085−4088.